

# Assignment of Amide $^1\text{H}$ and $^{15}\text{N}$ NMR Resonances in Detergent-Solubilized M13 Coat Protein: A Model for the Coat Protein Dimer<sup>†</sup>

Gillian D. Henry and Brian D. Sykes\*

Department of Biochemistry and MRC Group in Protein Structure and Function, University of Alberta,  
Edmonton, Alberta T6G 2H7, Canada

Received November 27, 1991; Revised Manuscript Received March 10, 1992

**ABSTRACT:** The major coat protein of the filamentous coliphage M13 is a 50-residue integral membrane protein. Detergent-solubilized M13 coat protein is a promising candidate for structure determination by nuclear magnetic resonance methods as the protein can be prepared in large quantities and the protein-containing micelle is reasonably small. Under the conditions of our experiments, SDS-bound coat protein exists as a dimer with an apparent molecular weight of 27 000. Broad lines and poor resolution in the  $^1\text{H}$  spectrum have led us to adopt an  $^{15}\text{N}$ -directed approach, in which the coat protein was labeled both uniformly with  $^{15}\text{N}$  and selectively with [ $\alpha$ - $^{15}\text{N}$ ]alanine, -glycine, -valine, -leucine, -isoleucine, -phenylalanine, -lysine, -tyrosine, and -methionine. Nitrogen resonances were assigned as far as possible using carboxypeptidase digestion, double-labeling, and an independent knowledge of the amide proton exchange rates determined from neighboring assigned  $^{13}\text{C}$ -labeled carbonyl carbons.  $^1\text{H}/^{15}\text{N}$  heteronuclear multiple quantum coherence (HMQC) spectroscopy of both uniform and site-selectively-labeled proteins subsequently correlated amide nitrogen with amide proton chemical shifts, and the assignments were completed sequentially from homonuclear NOESY and HMQC–NOESY spectra. The most slowly exchanging amide protons were shown to occur in a continuous stretch extending from methionine-28 to phenylalanine-42. This sequence includes most of the resonances of the hydrophobic core, although it is shifted toward the C-terminal end of the protein. Strong NH to NH ( $i, i+1$ ) nuclear Overhauser enhancements are a feature of the coat protein, which appears to be largely helical. Between 20 and 25 residues give rise to 2 juxtaposed resonances which can be seen clearly in the HMQC spectrum of uniform  $^{15}\text{N}$ -labeled coat protein. These residues are concentrated in a region extending from the beginning of the membrane-spanning sequence through to the disordered region near the C-terminus. We propose that dodecyl sulfate-bound M13 coat protein consists of two independent domains, an N-terminal helix which is in a state of moderately fast dynamic flux and a long, stable, C-terminal membrane-spanning helix, which undergoes extensive interactions with a second monomer. Amide  $^1\text{H}$  chemical shifts are consistent with this picture; in addition, a marked periodicity is observed at the C-terminal end of the molecule.

**A**lthough the amino acid sequences of many integral membrane proteins are known, detailed structural information is available in only two cases: bacteriorhodopsin (Henderson & Unwin, 1975; Henderson et al., 1990) and the *Rhodospseudomonas* photosynthetic reaction center (Deisenhofer et al., 1985). Bacteriorhodopsin forms a two-dimensional crystalline lattice in the native membrane, allowing a three-dimensional structure to be built by reconstruction of images obtained with the electron microscope. Seven  $\alpha$ -helices run perpendicular to the bilayer and correspond to apolar segments in the amino acid sequence of the protein (Engelman et al., 1982). More recently, the photosynthetic reaction center of *Rhodospseudomonas viridis* was crystallized in detergent (*N,N*-dimethyldodecylamine *N*-oxide; Michel, 1982) and the structure solved to 3-Å resolution by X-ray diffraction. Each of the 11 membrane-spanning segments is  $\alpha$ -helical and consists predominantly of hydrophobic amino acid residues. By necessity, bacteriorhodopsin and the photosynthetic reaction center have heavily influenced our concepts of membrane protein structure. Although numerous algorithms have been developed to predict the location of membrane-spanning helices, and these have received widespread application, their success remains difficult to judge, and the situation serves to illustrate the requirement for more structural information (Fasman & Gilbert, 1990; Jähnig, 1990). A second class of intrinsic membrane proteins

is also known to exist. Porin, which forms voltage-dependent channels in the outer membrane of *Escherichia coli*, does not possess apolar domains and consists largely of an antiparallel  $\beta$ -pleated sheet (Kleffel et al., 1985; Weiss et al., 1991).

Nuclear magnetic resonance (NMR) spectroscopy has been used to determine the structures of numerous small soluble proteins (usually less than 100 residues; Wüthrich, 1989). In principle, NMR techniques are equally applicable to membrane proteins; the problems lie with solubility and size. Membrane proteins can often be solubilized in detergent micelles, thereby alleviating the first problem (Tanford & Reynolds, 1976); however, the micelle-bound proteins tumble slowly in solution, leading to broad resonance lines, and in turn to weak or missing cross-peaks in two-dimensional spectra. The successful application of NMR spectroscopy to the "solution" structures of membrane proteins will therefore require a moderately small protein which can be solubilized effectively in small micelles. A worthwhile candidate is the major coat protein of the *E. coli* phage M13, which is only 50 residues long (van Wezenbeek et al., 1980). M13 coat

<sup>†</sup>Supported by the Medical Research Council of Canada (MRC Group in Protein Structure and Function).

<sup>1</sup> Abbreviations: NMR, nuclear magnetic resonance; NOE, nuclear Overhauser enhancement; ppm, parts per million; pH\*, pH meter reading uncorrected for deuterium isotope effects; SDS, sodium dodecyl sulfate; SDS- $d_{25}$ , perdeuterated sodium dodecyl sulfate; COSY, two-dimensional *J*-correlated spectroscopy; DQF, double quantum filter; HMQC, heteronuclear multiple quantum coherence; HOHAHA, two-dimensional homonuclear Hartman–Hahn spectroscopy; NOESY, two-dimensional nuclear Overhauser enhancement spectroscopy.

protein is also a popular model system for the study of membrane assembly (Wickner, 1980, 1988; Kuhn et al., 1990), so its structure is of general interest.

Bacteriophage M13 is a simple nucleoprotein particle, consisting of a single-stranded DNA circle encapsulated by 2700 copies of the major coat protein to form a characteristic long filament (Marvin & Wachtel, 1975; Makowski, 1984). Although the phage particles do not contain lipid, the coat protein is deposited as a transmembrane protein in the inner membrane of the *E. coli* host upon infection (Smilowitz et al., 1972). New coat protein molecules, synthesized with a 23-residue leader sequence, also insert into the inner membrane whereupon the signal sequence is removed by host-encoded leader peptidase (Chang et al., 1978). Phage assembly takes place within the inner membrane as the progeny phage are extruded into the surrounding medium. The phage can be isolated easily and provide large quantities of coat protein.

M13 coat protein comprises an acidic N-terminal sequence, a 19-residue highly hydrophobic region, and a short basic C-terminus (Figure 8). It spans the bilayer once, with the C-terminus on the cytoplasmic side of the membrane and the N-terminus directed toward the periplasmic space (Wickner, 1975). The protein must adapt itself to two distinct environments: in its structural role, it undergoes extensive protein-protein interactions in the lipid-free environment of the phage, yet during infection it spans the hydrophobic bilayer of the *E. coli* membrane without disrupting the host cells which continue to grow and divide. Circular dichroism, laser Raman spectroscopy, X-ray fiber diffraction, and solid-state NMR experiments suggest the coat protein of intact phage to be almost fully helical ( $\alpha$  or a-form) whereas a second, distinct conformation which seems to possess less helical structure (the 50%  $\alpha$  or b-form) is reported to exist in detergent micelles (e.g., sodium dodecyl sulfate, sodium deoxycholate) or phosphatidylcholine vesicles. Under certain conditions, an oligomeric or polymeric  $\beta$ -sheet structure (the c-form) is also observed (Nozaki et al., 1976, 1978; Williams & Dunker, 1977; Marvin & Wachtel, 1976; Makowski, 1984; Opella et al., 1987; Spruijt et al., 1989). Most NMR experiments so far have concentrated on coat protein dynamics [e.g., see Cross and Opella (1981), Dettman et al. (1982, 1984), Leo et al. (1985), Henry et al. (1986, 1987a,b), Bogusky et al. (1985, 1988), and Henry and Sykes (1990a,b)] although a two-dimensional NMR study of the coat protein of the related phage Pf1 demonstrates the presence of substantial  $\alpha$ -helical structure (Schiksnis et al., 1988; Shon et al., 1991).

In either sodium deoxycholate or sodium dodecyl sulfate (SDS) micelles, sedimentation equilibrium experiments have shown the protein to be a dimer (Makino et al., 1976; Cavalieri et al., 1976), and it has been suggested that the dimer is both parallel and asymmetric (Henry & Sykes, 1990c). Previous experiments, using a variety of detergents, have shown SDS-solubilized protein to yield the narrowest lines, most suitable for two-dimensional NMR (Henry & Sykes, 1990a). SDS does not appear to be denaturing to small hydrophobic proteins (Nozaki et al., 1978). Under ionic strength conditions similar to those of our experiments, the coat protein dimer was shown to bind 60 molecules of SDS (Makino et al., 1976; Cavalieri et al., 1976) to form a complex of approximately 27 000 molecular weight.

The first step in structure determination by NMR spectroscopy is resonance assignment. Standard procedure requires the recognition of amino acid spin systems (in a COSY or HOHAHA experiment) followed by the establishment of sequential connectivities on the basis of characteristic NOEs

between NH,  $\text{C}_\alpha\text{H}$ , and  $\text{C}_\beta\text{H}$  protons of adjacent residues (Billeter et al., 1982). However, experiments such as COSY and HOHAHA, which rely on homonuclear  $J$  couplings, do not work well with larger molecules when the line widths approach the value of the coupling constant, and an alternative approach must be undertaken for resonance assignment. We have adopted the following strategy: (i) the protein was labeled both uniformly and at selective sites with  $^{15}\text{N}$  (Cross & Opella, 1985; Bogusky et al., 1985, 1988; Henry & Sykes, 1990b); (ii) the  $^{15}\text{N}$  spectra were assigned directly as far as possible; (iii) attached protons were assigned using  $^1\text{H}/^{15}\text{N}$  heteronuclear shift correlation (HMQC; Müller, 1979; Bax et al., 1983), yielding numerous starting points for the interpretation of NOESY data; (iv) sequential connectivities in both homonuclear and heteronuclear NOESY experiments readily established the identity of remaining  $^1\text{H}$  and  $^{15}\text{N}$  resonances. The amide nitrogen and proton resonances of M13 coat protein were assigned in this way, without any preexisting knowledge of  $\text{C}_\alpha\text{H}$  or  $\text{C}_\beta\text{H}$  chemical shifts. Similar methods have been used with other large proteins such as staphylococcal nuclease (Torchia et al., 1988, 1989),  $T_4$  lysozyme (McIntosh et al., 1990), and the micelle-bound coat protein of Pf1 (Schiksnis et al., 1988). All of the amide proton and nitrogen resonances in SDS-bound M13 coat protein have been assigned. This has enabled us to interpret NOESY spectra, to identify the slowly exchanging amide protons, and to investigate the nature of the association between the coat protein monomers.

## EXPERIMENTAL PROCEDURES

### Materials

Auxotrophic *Escherichia coli* strains G11a1 (CGSC 5168, Hfr, rel A1, ilv 229, met B1, amp A1), AT2457 (CGSC 4507, Hfr, thi 1, gly A6, rel A1,  $\lambda^-$ , spo T1), AT2471 (CGSC 4510, Hfr, thi 1, tyr A4, rel 1,  $\lambda^-$ ), and KA197 (CGSC 5243, Hfr, thi 1, phe A97, rel A1,  $\lambda^-$ ) were obtained from Barbara Bachmann, *E. coli* Genetic Stock Centre, Yale University School of Medicine.  $^{15}\text{N}$ -Glycine, L- $^{15}\text{N}$ -leucine, DL- $^{15}\text{N}$ -valine, DL- $^{15}\text{N}$ -phenylalanine, DL- $^{15}\text{N}$ -tyrosine, DL- $^{15}\text{N}$ -lysine, L- $^{15}\text{N}$ -alanine, L- $^{13}\text{C}$ -phenylalanine, and L- $^{13}\text{C}$ -lysine (all 99 atom %) and perdeuterated sodium dodecyl sulfate (99.4%) were obtained from MSD Isotopes (Pointe Claire, Quebec). L- $^{15}\text{N}$ -Methionine and L- $^{15}\text{N}$ -isoleucine (99%) were from Cambridge Isotopes (Woburn, MA), and  $(^{15}\text{NH}_4)_2\text{SO}_4$  (99.7%) was from Isotec Inc. (Miamisburg, OH). Carboxypeptidases A and B (both treated with diisopropyl fluorophosphate) were obtained from Sigma (St. Louis, MO).

### Methods

**Growth of Labeled Phage.** Labeled M13 was grown in M63 minimal medium (Miller, 1972) supplemented as described by Henry and Sykes (1990b). Auxotrophic *E. coli* K12 strains were used for glycine (AT2457), tyrosine (AT2471), phenylalanine (KA197), and leucine, isoleucine, valine, and methionine (G11a1) labels. Double-labeled phage preparations ( $[1\text{-}^{13}\text{C}]\text{phenylalanine}/[\alpha\text{-}^{15}\text{N}]\text{lysine}$  and  $[1\text{-}^{13}\text{C}]\text{lysine}/[\text{phenylalanine}]^{15}\text{N}$ ) were grown with the phenylalanine auxotroph KA197. Strain G11a1 was used when an auxotroph was not available (alanine and lysine). Transamination was negligible, even in the absence of an auxotrophic strain. Uniform  $^{15}\text{N}$ -labeled phage was prepared with a nonauxotrophic strain of *E. coli* grown on M63 minimal medium with  $(^{15}\text{NH}_4)_2\text{SO}_4$  as the sole nitrogen source.

**Preparation of NMR Samples.** SDS-solubilized coat protein was prepared as described by Henry et al. (1986). The phage DNA was removed by gel filtration on Sephacryl S200

Table I:  $^{15}\text{N}$  and  $^1\text{H}$  Assignments for SDS-Solubilized M13 Coat Protein, pH 4.5, 45 °C

residue	nitrogen (ppm)	proton (ppm)	residue	nitrogen (ppm)	proton (ppm)
Ala-1	42.6 <sup>a</sup>		Ala-25	123.5	8.02
Glu-2	122.0	8.59	Trp-26	117.25, 118.0	7.91, 8.12
Gly-3	112.1	8.35	(side chain)	129.3, 129.0	9.65, 9.63
Asp-4	120.9	8.03	Ala-27	122.4, 122.9	7.71, 7.52
Asp-5	120.8	8.32	Met-28	116.9	7.83, 7.76
Pro-6	138.7 <sup>a</sup>		Val-29	120.5 <sup>b</sup>	7.92, 7.87 <sup>b</sup>
Ala-7	122.4	8.08	Val-30	120.3 <sup>b</sup>	7.99, 7.92 <sup>b</sup>
Lys-8	119.4	7.61	Val-31	120.1 <sup>b</sup>	8.01, 7.94 <sup>b</sup>
Ala-9	123.5	8.01	Ile-32	121.0	8.20
Ala-10	123.5	8.01	Val-33	124.3, 123.7	8.78, 8.71
Phe-11	119.9	8.21	Gly-34	109.6	8.93
Asn-12	119.0	8.38	Ala-35	124.0, 124.7	8.88, 8.84
(side chain)					
	113.2	7.49	Thr-36	115.9, 115.7	8.00, 7.93
		6.85	Ile-37	122.0	8.28, 8.30
Ser-13	117.8	7.98	Gly-38	109.2, 109.1	8.74
Leu-14	124.8	7.89	Ile-39	123.3	8.68, 8.58
Gln-15	120.1	8.09	Lys-40	121.3	8.09, 8.01
(side chain)					
	112.9	6.97	Leu-41	121.5, 121.3	8.79, 8.70
		6.60	Phe-42	123.2	8.89, 8.83
Ala-16	122.8	7.72	Lys-43	121.4, 121.1	8.68, 8.60
Ser-17	115.3	7.78	Lys-44	122.3	7.91
Ala-18	126.3	8.18	Phe-45	119.8	8.41
Thr-19	111.3	7.76	Thr-46	111.1, 111.2	7.87
Glu-20	122.5	7.89	Ser-47	118.7	7.58
Tyr-21	119.0	7.71	Lys-48	124.2, 124.1	7.71, 7.65
Ile-22	121.1, 120.8	7.56, 7.50	Ala-49	126.6	7.94
Gly-23	110.6, 110.8	8.19, 8.16	Ser-50	121.7	7.76
Tyr-24	120.1	7.63			

<sup>a</sup> Assigned by Bogusky et al. (1988). <sup>b</sup>  $^1\text{H}$  frequencies obtained from the NOESY spectrum. These  $^{15}\text{N}$  frequencies are approximate.

SF (Woolford & Webster, 1975) equilibrated in 5 mM sodium borate, pH 9.0, 90 mM sodium chloride, and 10 mM SDS. Perdeuterated SDS (SDS- $d_{25}$ ) was used for  $^1\text{H}$  NMR samples. Protein-containing fractions from the column were pooled and concentrated to about 3.6 mL ( $^{15}\text{N}$  samples) or 0.6 mL ( $^1\text{H}$  samples) by ultrafiltration. Samples to be run in  $^2\text{H}_2\text{O}$  were freeze-dried after the pH was adjusted to 7.5; they were then taken up in a  $^2\text{H}_2\text{O}$  solution containing 10 mM acetic acid- $d_4$  plus a small amount of  $^2\text{HCl}$ , and the pH\* was rapidly adjusted to 4.5 if necessary. pH\* values measured in  $^2\text{H}_2\text{O}$  are direct meter readings. The freeze-drying procedure does not affect the NMR spectrum (O'Neil & Sykes, 1988). Samples in which the slowly exchanging protons were selectively deuterated were prepared similarly, except that the pH\* was adjusted to 9.0 and the sample was left at room temperature overnight to ensure complete exchange. The pH was then readjusted to 7.5, and the sample was freeze-dried and redissolved in  $\text{H}_2\text{O}$  buffer at pH 4.5 as described above.  $^1\text{H}$  NMR samples to be run in  $\text{H}_2\text{O}$  were prepared by direct addition of  $^2\text{H}_2\text{O}$  (10% final volume) to provide the field-frequency lock and acetic acid- $d_4$  buffer (10 mM final concentration), and the pH was adjusted to 4.5.  $^{15}\text{N}$  samples were also made 10%  $^2\text{H}_2\text{O}$  by addition of an appropriately buffered solution. The protein concentration was about 2.5 mM in all samples.

**NMR Spectroscopy.** All spectra were acquired at 45 °C and pH 4.5 unless otherwise stated.  $^{15}\text{N}$  NMR spectra were recorded at 30.4 MHz on a Nicolet NT 300 WB NMR spectrometer equipped with a 12-mm  $^{15}\text{N}$  probe. INEPT spectra were acquired using the refocused decoupled INEPT pulse sequence (Morris, 1980) with the delays adjusted for secondary amides. The decoupled DEPT spectrum (Doddrell et al., 1982) was recorded with a final 90° pulse. The acquisition time and the delay between transients were both 1 s. The one-bond coupling constant,  $J_{\text{NH}}$  was taken to be 94.5

Hz (the value measured for *N*-acetylglycine) throughout these experiments.

$^1\text{H}$  NMR spectra were recorded on a Varian VXR 500 NMR spectrometer operating at a frequency of 500 MHz for  $^1\text{H}$  and 50.7 MHz for  $^{15}\text{N}$ . In all two-dimensional experiments, quadrature detection in  $t_1$  employed the hypercomplex method of States et al. (1982), and water or residual  $^1\text{H}^2\text{HO}$  was suppressed by presaturation (2.0–2.2 s).  $^1\text{H}/^{15}\text{N}$  heteronuclear multiple quantum coherence spectra (HMQC; Bax et al., 1983) were acquired with  $^{15}\text{N}$  decoupling during the acquisition period (WALTZ-16; Shaka et al., 1983); spectra were collected with 1024 real data points in the  $t_2$  dimension and 256 increments in  $t_1$ . Data were zero-filled to 2048 ( $^1\text{H}$ ) and 1024 ( $^{15}\text{N}$ ) points and processed with mild resolution enhancement. The  $^1\text{H}$  observe and  $^{15}\text{N}$  sweep widths were 5022 and 3000 Hz, respectively, leading to a digital resolution of 0.01 ppm for  $^1\text{H}$  and 0.25 ppm for  $^{15}\text{N}$ . An additional spectrum of uniform  $^{15}\text{N}$ -labeled protein was recorded with high digital resolution in the  $^{15}\text{N}$  dimension in order to obtain the chemical shifts presented in Table I. Chemical shifts were referenced with respect to internal sodium 2,2-dimethyl-2-silapentane-5-sulfonate for  $^1\text{H}$  and to 1 M  $\text{NH}_4\text{Cl}$  in 2 M  $\text{HCl}$  (external standard) for  $^{15}\text{N}$ .  $^{15}\text{N}$  chemical shifts were then adjusted to a liquid ammonia reference frequency at 0 ppm according to Srinivasan and Lichter (1977). Phase-sensitive NOESY spectra were recorded with 256  $t_1$  increments, using mixing times of 50 and 100 ms in  $\text{H}_2\text{O}$  and  $^2\text{H}_2\text{O}$  and at 200 ms in  $\text{H}_2\text{O}$  alone. The final data matrix was zero-filled to 2048 by 2048 real points. The HMQC–NOESY spectrum (Shon & Opella, 1989) was acquired with a mixing time of 100 ms under conditions similar to those of the HMQC spectra.

## RESULTS

**$^1\text{H}$  NMR Spectroscopy.** As the coat protein–SDS complex is relatively large, NMR spectra were recorded at elevated

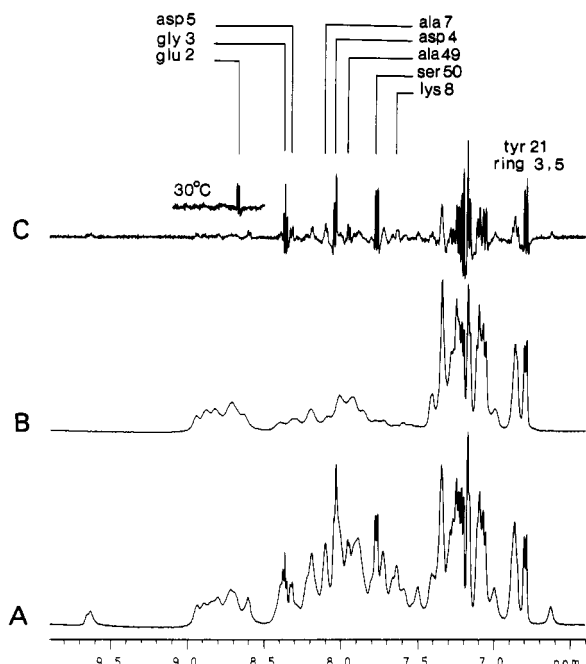


FIGURE 1:  $^1\text{H}$  NMR spectra of the amide and aromatic region of 2.5 mM M13 coat protein in SDS- $d_{25}$  micelles, 5 mM sodium borate, 90 mM NaCl, and 10 mM acetic acid- $d_4$ , pH 4.5, 45  $^\circ\text{C}$ . (A) Spectrum recorded in  $\text{H}_2\text{O}$  solution; 128 transients, 0.5-Hz line broadening. (B) Spectrum recorded after 2 h of equilibration in buffered  $^2\text{H}_2\text{O}$  solution; 128 transients, 0.5-Hz line broadening. The spectra in (A) and (B) were normalized with respect to the ring 3,5-protons of tyrosine-21. (C) Data from (A), weighted with a strong resolution enhancement function to emphasize the very narrow lines, which arise from particularly mobile residues. The assignments of some of the more mobile resonances (obtained by alignment with the HMQC spectrum which was assigned as described in the text) are indicated. Above is a small region of the spectrum recorded at 30  $^\circ\text{C}$ , showing the narrow amide proton resonance of glutamic acid-2. This resonance is largely saturated at 45  $^\circ\text{C}$  when the rate of exchange of the amide proton with the solvent is faster (see text).

temperature (45  $^\circ\text{C}$ ) to reduce the overall rotational correlation time. Since some of the amide protons exchange quite rapidly with the solvent (Henry et al., 1987b; O'Neil & Sykes, 1988), data were collected at pH 4.5, close to the rate minimum (Englander & Kallenbach, 1984; Henry & Sykes, 1990b). The only exceptions are some of the  $^{15}\text{N}$  assignment experiments. The amide and aromatic region of the 500-MHz  $^1\text{H}$  NMR spectrum of M13 coat protein in perdeuterated SDS micelles (SDS- $d_{25}$ ) in  $^1\text{H}_2\text{O}$  is shown in Figure 1A. None of the amide protons are resolved except for two of the side chain amides; the most downfield resonance is the tryptophan-26 indole proton, and the most upfield peak is the  $\text{H}_2$  proton of glutamine-15 (Cross & Opella, 1981; O'Neil & Sykes, 1990). In  $^2\text{H}_2\text{O}$ , many of the amide protons are lost after only 2 h at 45  $^\circ\text{C}$  (Figure 1B), but most of the rest form a stable set which survive for several weeks (O'Neil & Sykes, 1988). Several residues in M13 coat protein have been observed to possess substantial motional freedom (Cross & Opella, 1980; Henry & Sykes, 1986, 1987a; Bogusky et al., 1988). These are apparent as narrow lines, with noticeable spin coupling, superimposing the broad resonance envelope of the amide protons in Figure 1A; they can be observed most clearly when these data are multiplied by a strong resolution enhancement function (Figure 1C). The triplet, which must be a glycine resonance as it is coupled to two  $\alpha$ -protons, can be identified immediately as glycine-3 NH as the  $^{13}\text{C}$  carbonyl and  $^{15}\text{N}$  amide resonances of glycine-3 are already known to be exceptionally narrow (Henry et al., 1987a; Bogusky et al., 1988).

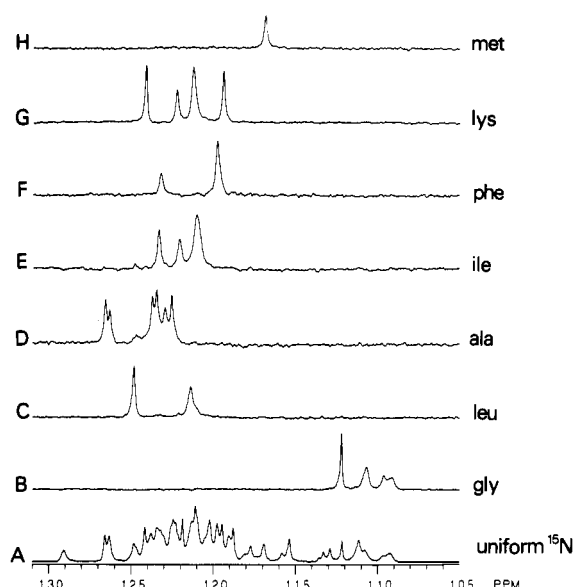
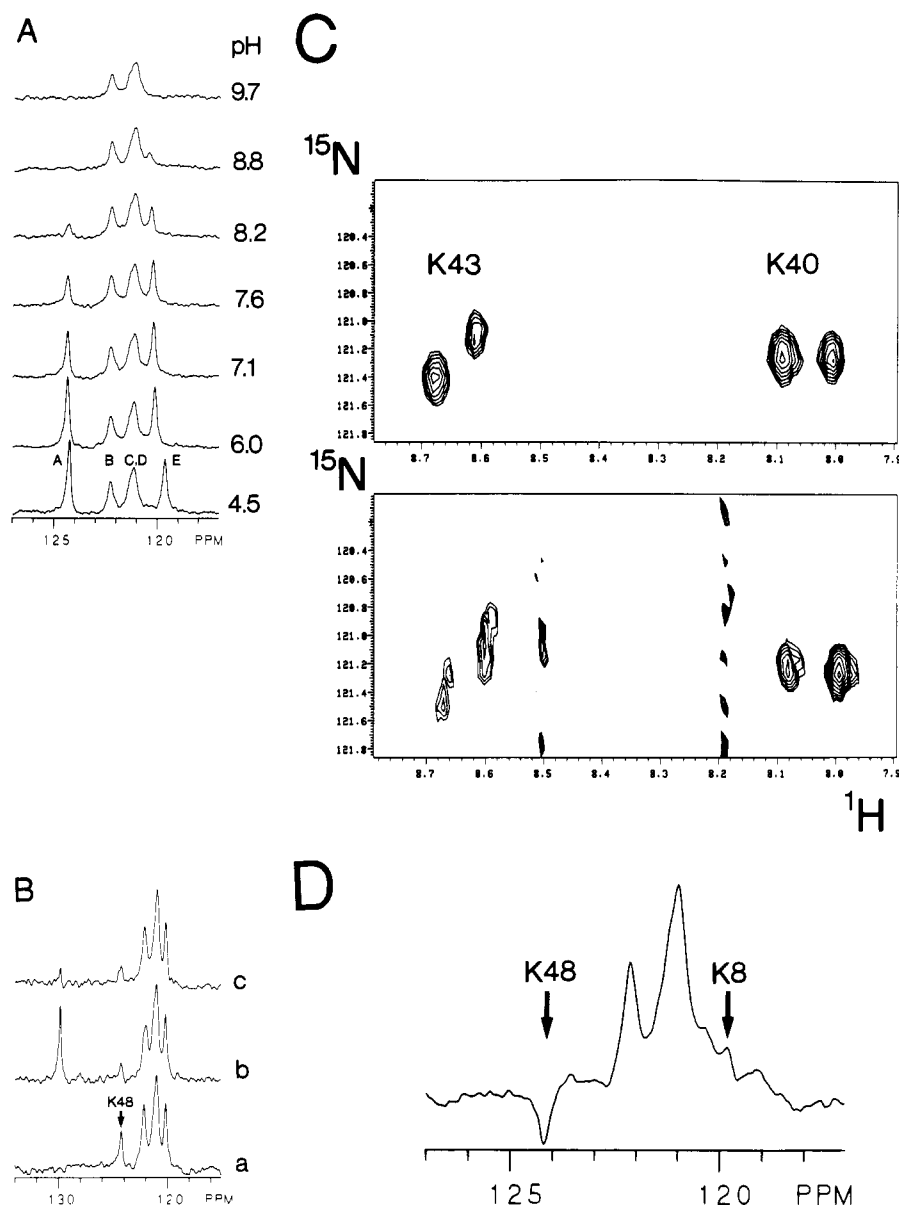


FIGURE 2: Proton-decoupled DEPT (A) and INEPT (B-H)  $^{15}\text{N}$  NMR spectra of uniformly- and site-selectively-labeled M13 coat protein in SDS micelles at 45  $^\circ\text{C}$ , pH 4.5. The acquisition time and the delay between transients were both 1 s. (A) Uniformly-labeled protein (4136 transients); (B) glycine (23 584 transients); (C) leucine (12 432 transients); (D) alanine (5000 transients); (E) isoleucine (5000 transients); (F) phenylalanine (3696 transients); (G) lysine (2496 transients); (H) methionine (5000 transients). Representative spectra of tyrosine- and valine-labeled coat protein can be found in Henry and Sykes (1990b).

**$^{15}\text{N}$  NMR Spectroscopy.** Individual site-specific  $^{15}\text{N}$  labels are easily introduced into the coat protein (Cross & Opella, 1985). The  $^{15}\text{N}$  INEPT spectra (pH 4.5, 45  $^\circ\text{C}$ ) of 7 such labeled proteins, glycine (4 residues), leucine (2 residues), alanine (10 residues), isoleucine (4 residues), phenylalanine (3 residues), lysine (5 residues), and methionine (1 residue), are shown in Figure 2 with the spectrum of protein labeled uniformly with  $^{15}\text{N}$  presented for comparison. Scrambling of the label is insignificant; however, the extent of incorporation of the labeled amino acids is variable. Isoleucine, for example, labels relatively poorly whereas the incorporation of lysine is excellent. Assignment of the  $^{15}\text{N}$  resonances will ultimately enable us to assign the amide proton spectrum. Fortunately, the  $^{15}\text{N}$  spectra are relatively easy to assign, and a few resonances have been identified already (Bogusky et al., 1988; Henry et al., 1990b). We have used three different methods: prior knowledge of the amide exchange rate, carboxypeptidase digestion, and double-labeling of the peptide bond with  $^{13}\text{C}$  and  $^{15}\text{N}$ . All these techniques can be illustrated with the five lysine amide nitrogens (residues 8, 40, 43, 44, and 48). The peaks are labeled A-E in Figure 3A for convenience.

**(A) Amide Exchange.** Amide exchange rates in M13 coat protein are known in some detail from  $^1\text{H}$ -detected "exchange out" experiments in  $^2\text{H}_2\text{O}$  buffer (O'Neil & Sykes, 1988) and from  $^{13}\text{C}$  NMR experiments with labeled peptide carbonyls. A peptide carbonyl carbon undergoes a small two-bond isotope shift upon deuteration of the adjacent nitrogen atom (Feeney et al., 1974), and this can be exploited to measure the hydrogen exchange rate (Henry et al., 1987b; Henry and Sykes, unpublished results). The carbonyl carbon of phenylalanine-42 reflects exchange at the lysine-43 amide so that in a small protein like M13, a carbonyl assignment can often be translated unambiguously into an amide nitrogen assignment if the exchange rate can be determined independently. The decoupled INEPT experiment is sensitive to exchange as it effectively transfers magnetization to an insensitive nucleus ( $^{15}\text{N}$ ) from the attached (coupled) proton. When the rate of ex-



**FIGURE 3:** Assignment of lysine residues. (A) pH titration of  $[\alpha\text{-}^{15}\text{N}]$ lysine-labeled coat protein in SDS micelles. Spectra were recorded with the decoupled INEPT pulse sequence at 23 °C, and 1000 transients were averaged; conditions otherwise as in Figure 2. (B) Assignment of lysine-48 by carboxypeptidase digestion. (a)  $^{15}\text{N}$  INEPT spectrum of  $[\alpha\text{-}^{15}\text{N}]$ lysine-labeled coat protein, pH 8.0. Two lysine residues (lysines-48 and -8, peaks A and E) are reduced in intensity at this pH due to amide exchange with the solvent. (b) Spectrum recorded after addition of carboxypeptidase A (0.65 mg) which removes alanine-49 and serine-50, leaving lysine-48 (peak A) as the new C-terminal residue. The intensity of the new resonance is greater than the original because inductive effects from the negatively charged carboxyl slow down the exchange rate of the C-terminal amide. (c) After addition of carboxypeptidase B (2 mg), which removes lysine-48. The resonance of the free amino group does not appear in the INEPT spectrum. (C) Assignment of lysine-44 from two-dimensional  $^1\text{H}/^{15}\text{N}$  HMQC spectra. Only the region expanded around lysines-C (K43) and -D (K40) is shown. (Top)  $[\alpha\text{-}^{15}\text{N}]$ lysine-labeled coat protein; (bottom)  $[1\text{-}^{13}\text{C}]$ phenylalanine/ $[\alpha\text{-}^{15}\text{N}]$ lysine-labeled coat protein, showing carbon/nitrogen spin coupling across the unique phenylalanine-42-lysine-43 peptide bond. Both spectra were subject to a strong resolution enhancement function in order to resolve the small coupling (about 14 Hz). (D) Directly detected  $^{15}\text{N}$  NMR spectrum of  $[\alpha\text{-}^{15}\text{N}]$ lysine-labeled coat protein, pH 5.7, showing the  $^{15}\text{N}$  NOE; lysine-48 has a negative NOE, and lysine-8 is nulled. The decoupler was gated on during acquisition only; 9700 transients were averaged, and the delay between transients was 3 s.

change approaches the relaxation rate of the amide proton ( $\sim 2\text{ s}^{-1}$  in M13), the observed signal intensity is reduced by transfer of saturation from water unless the delay between transients is significantly longer than the  $T_1$  of water (Henry & Sykes, 1990b). Since amide exchange is catalyzed by  $\text{OH}^-$  ions, the exchange rates of the more labile amides can be brought into the  $2\text{-s}^{-1}$  "window" by increasing the pH, as shown in Figure 3A. On the time scale of this experiment, the amide protons of residues A and E exchange much more quickly than B, C, or D. Resonance E shifts downfield slightly as the pH increases (presumably reflecting titration of a nearby carboxyl), but the frequencies of other resonances are not affected. From  $^{13}\text{C}$  experiments, it is known that lysines-43 and -44 exchange

slowly on this time scale and at about the same rate as each other (Henry et al., 1987b). The rates of lysine-8 and lysine-48 are not known for certain, but the adjacent amides (alanine-7, alanine-9, and alanine-49) are among the fastest in the protein, and peaks A and E exchange at comparable rates. Lysines-8 and -48 therefore correspond to resonances A and E. Similarly, although the exchange rate of lysine-40 has not been measured directly, phenylalanine-42, leucine-41, and isoleucine-39 are among the slowest amides in the protein (Henry et al., 1987b; Henry & Sykes, 1990b; also see later). Rates of slowly exchanging amides can be measured by dissolving protonated protein in buffered  $^2\text{H}_2\text{O}$  and monitoring the time-dependent disappearance of the INEPT signal (Henry

et al., 1990b). At pH\* 6.1, peak B and half of the C,D peak (arbitrarily designated C) exchange very quickly, and these two resonances were assigned to lysines-43 and -44. Peak D, which exchanges more slowly, must therefore correspond to lysine-40 (data not shown, but see Figure 4B).

**(B) Carboxypeptidase Digestion.** Lysine-48 was assigned definitively by carboxypeptidase digestion. Carboxypeptidase A cleaves serine-50 and alanine-49 sequentially from the C-terminus of the protein, but it will not remove a basic residue (lysine-48) which becomes the new C-terminal residue. Figure 3B(a) shows the protein at pH 8.0 before digestion. After treatment with carboxypeptidase A [Figure 3B(b)], the intensity of resonance A (lysine-48) is greatly reduced, and a new peak is observed at 129.8 ppm. The rest of the spectrum is unaltered. Further digestion with carboxypeptidase B (which removes only basic residues) eliminates the terminal lysine [Figure 3B(c)]. Resonance A can now be assigned to lysine-48 with complete confidence, so resonance E must be lysine-8. In principle, the carboxypeptidase A/B cycles could be continued indefinitely, as the enzymes are quickly inactivated in SDS solution; however, digestion proceeds at a negligible rate once the unstructured terminal residues are removed.

**(C) Double-Labeling.** Lysines-43 and -44 were identified by preparing  $[1-^{13}\text{C}]$ phenylalanine/ $[\alpha-^{15}\text{N}]$ lysine-labeled phage in which the unique phenylalanine-42-lysine-43 peptide bond was revealed by carbon-nitrogen spin coupling ( $^1J_{\text{NC}} \approx 14$  Hz). This required a two-dimensional  $^1\text{H}/^{15}\text{N}$  HMQC experiment [e.g., see Torchia et al. (1988)] and strong resolution enhancement (Figure 3C) but confirmed peak C as residue 43 and, by elimination, peak B as residue 44. It has been observed previously that three of the lysine residues give rise to two distinct resonances (Henry & Sykes, 1990c) and one of these is lysine-43. The carbon-nitrogen spin coupling thus appears superimposed upon a pair of resonances. This is a widespread phenomenon which will be discussed fully later. There remains a slight ambiguity over the identity of lysine-40 and lysine-8, the assignment of which did not rely on directly measured exchange rates. We have established a very useful starting point, however, and homonuclear NOESY and HMQC-NOESY readily established the assignment as correct (discussed later, see also Figures 6 and 7). The assignment of the lysine residues has been described in detail both because it is illustrative of our general approach and because our results differ substantially from those reported earlier (Bogusky et al., 1988). The gyromagnetic ratio of  $^{15}\text{N}$  is small and negative, resulting in a large negative  $^{15}\text{N}$  NOE when  $\omega\tau_c \ll 1$ . Protein spectra recorded in the presence of an  $^{15}\text{N}$  NOE are generally positive as  $\tau_c$  is large, but mobile residues will give rise to negative peaks. Such a negative NOE is observed for lysine-48 (Figure 3D), indicating the presence of substantial backbone motion in this region. The lysine-8 resonance is nulled in the presence of an  $^{15}\text{N}$  NOE and is thus more mobile than the C-terminal residues, lysines-40, -43, and -44. The fact that Bogusky et al. (1988) do not observe any negative NOEs may be a result of their higher operating field strength.

**(D) Other Assignments.** Both leucine and tyrosine residues have been assigned previously (Henry & Sykes, 1990b), and the methionine resonance obviously belongs to the single methionine-28. Isoleucine-22 was assigned on the basis of its fast exchange rate compared with the other isoleucines; this was known already from  $^{13}\text{C}$  carbonyl experiments on the neighboring residue, tyrosine-21 (Henry and Sykes, unpublished results; see also Figure 4a,b). Phenylalanines-11, -42, and -45 could be distinguished on the basis of known exchange rates (Henry et al., 1987b), and confirmation of the phenyl-

alanine-45 assignment was provided by preparation of  $[1-^{13}\text{C}]$ lysine/ $[^{15}\text{N}]$ phenylalanine-labeled protein (data not shown). Glycine-3 and the amino group of alanine-1 (which resonates well downfield of the amides) were assigned by Bogusky et al. (1988) on the basis of chemical shift (alanine-1) and strong negative NOEs. Alanine-49 was assigned by carboxypeptidase A digestion (not shown). The remaining alanine resonances were not assigned directly. We did not attempt to incorporate labeled serine, threonine, glutamic acid, glutamine, aspartic acid, asparagine, or tryptophan.

**$^1\text{H}/^{15}\text{N}$  HMQC Spectroscopy.** **(A) Backbone Amides.** Two-dimensional  $^1\text{H}/^{15}\text{N}$  HMQC spectroscopy can be used to correlate amide proton and amide nitrogen chemical shifts [e.g., see Griffey et al. (1985), Torchia et al. (1989), and McIntosh et al. (1990)] and also provides resolution of most of the overlapping resonances (Figure 4a; compare with Figure 1A). All of the protonated nitrogen atoms, with the possible exception of some of the primary amino groups, should be seen in the HMQC spectrum of uniform  $^{15}\text{N}$ -labeled coat protein. Contributions are to be expected from 48 backbone amides (i.e., not including the single proline) and the side chains of asparagine-12, glutamine-15, and tryptophan-26; however, a greater number of cross-peaks are obtained in practice. Equivalent HMQC spectra of the nine selectively labeled proteins (lysine, methionine, glycine, valine, isoleucine, leucine, alanine, phenylalanine, and tyrosine; Figure 5A-I) show that many residues such as isoleucine-22, methionine-28, and leucine-41 give rise to two resonances of approximately equal intensity. This feature has been noted before and ascribed to inequivalence of the subunits in the M13 coat protein dimer (Henry & Sykes, 1990c). Those resonances which have been identified in the  $^{15}\text{N}$  dimension up to this point are indicated in Figure 5, whereas the completed assignment is presented in Figure 4a. Figure 4b shows uniform  $^{15}\text{N}$ -labeled coat protein in  $^2\text{H}_2\text{O}$  buffer in which only the more slowly exchanging amides remain (O'Neil & Sykes, 1988). Data acquisition was begun 2 h after dissolution (as in Figure 2B) and took about 10 h to complete. Fifteen residues, including many of the "double" resonances, can be counted in the slowly exchanging group. Many of these may be identified as residues of the hydrophobic core by reference to the site-specifically-labeled proteins in Figure 5. Some of the amide exchange-based assignments discussed earlier can be seen easily by comparing spectra in Figure 5 with Figure 4b; for example, the slowly exchanging lysine-40 resonance is the only remaining lysine in  $^2\text{H}_2\text{O}$  buffer, whereas the rapidly exchanging isoleucine-22 is the only missing isoleucine resonance.

Some of the spectra in Figure 5 require comment. Three of the four valine resonances (Figure 5F) are poorly resolved in both dimensions of the HMQC spectrum. Similarly, three of the nine alanine amides result in one unresolved peak, although they are resolved to some extent in the one-dimensional spectrum (Figure 2D) due to better digital resolution. As an added complexity, two alanine residues give rise to two distinct resonances. These are the two more slowly exchanging alanine amides and can be seen quite clearly as the remaining alanine resonances in the HMQC spectrum uniformly-labeled coat protein is recorded in  $^2\text{H}_2\text{O}$  (Figure 4b; compare with the alanine-labeled protein in Figure 5G). The downfield "double" resonance belongs to the most slowly exchanging group of amide protons, whereas the upfield pair of resonances is partially exchanged with the solvent. The latter have an unusually large separation [0.19 ppm ( $^1\text{H}$ ) and 0.5 ppm ( $^{15}\text{N}$ )] and are indicated by arrows at their full intensities in Figure 5G. The initial intensities and distinctive amide exchange rates

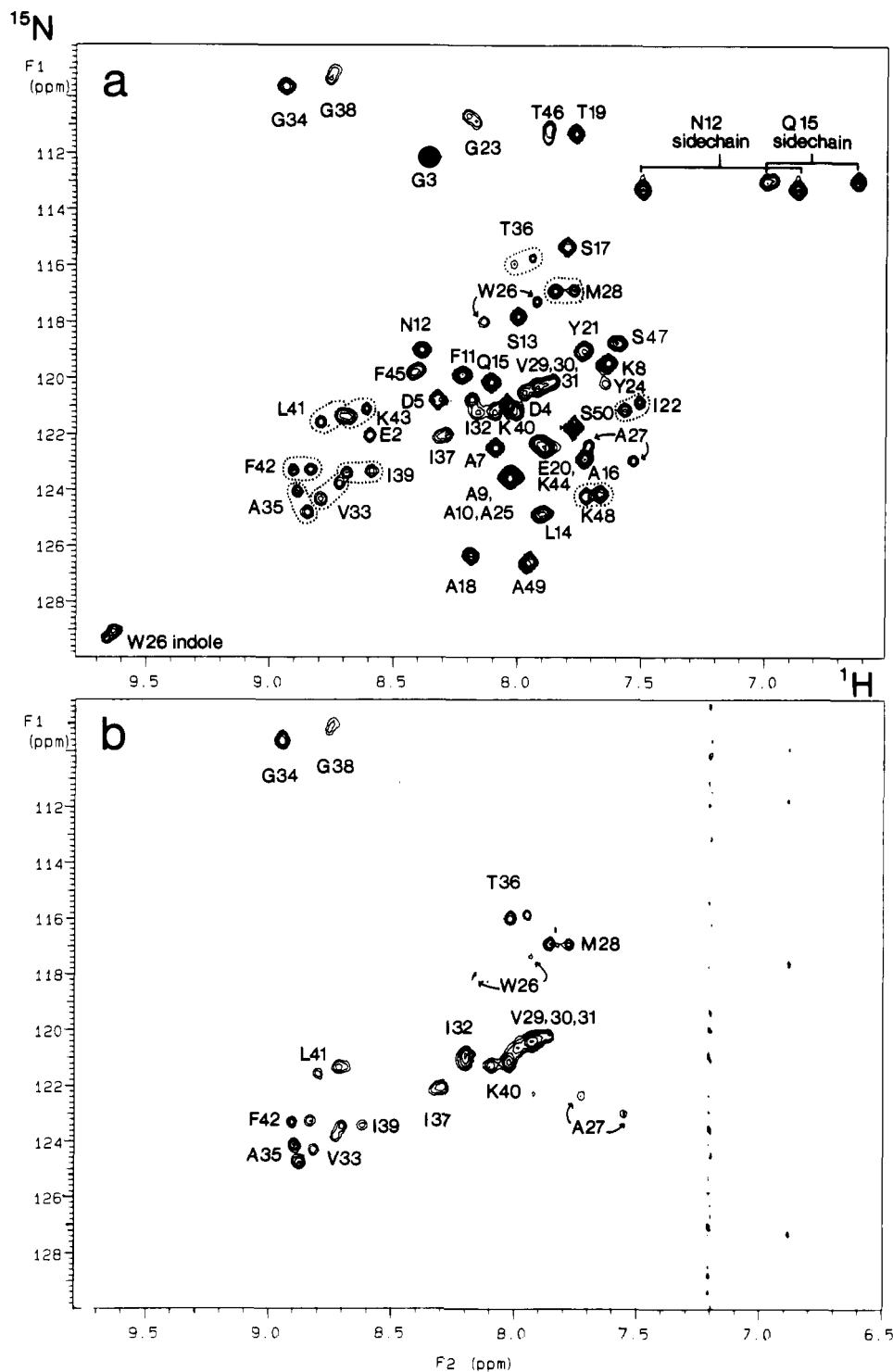


FIGURE 4: (a) Amide region of the  $^1\text{H}/^{15}\text{N}$  HMQC spectrum of uniformly  $^{15}\text{N}$ -labeled coat protein in  $\text{SDS-}d_{25}/\text{H}_2\text{O}$  buffer, pH 4.5, 45 °C, 32 transients/increment. (b) Equivalent spectrum in  $2\text{H}_2\text{O}$ ; acquisition was begun 2 h after dissolution (see Methods).

link each pair of alanine resonances to a single residue.

**(B) Side Chain Amides.** The single indole amide was assigned by Cross and Opella (1981) on the basis of its chemical shift. It is well-resolved in the HMQC spectrum of uniform  $^{15}\text{N}$ -labeled coat protein and also appears to undergo a small splitting in both dimensions. The primary amides of asparagine-12 and glutamine-15 are readily apparent in Figure 4A as the E and Z protons have different chemical shifts (Bundi & Wüthrich, 1979) but are both correlated to the same  $^{15}\text{N}$  atom. Asparagine and glutamine side chain amides were distinguished from the characteristic NOEs that are observed from the side chain amides to their own  $\beta$ - or  $\gamma$ -protons,

respectively (not shown). It is also possible to see the lysine side chain amino groups which resonate at a  $^1\text{H}$  frequency between 7.2 and 7.4 ppm and an  $^{15}\text{N}$  frequency of approximately 35 ppm (not shown). They are folded in the  $^{15}\text{N}$  dimension as the acquisition conditions were optimized for the observation of amide nitrogen frequencies.

**Sequential Assignments.** The 9  $^{15}\text{N}$  selectively-labeled proteins have enabled us to assign 34 of the 48 backbone amides at least to residue type, providing multiple firm starting points for the recognition of the characteristic NOEs which form the basis of the sequential assignment procedure (Billeter et al., 1982; Englander & Wand, 1987). Using the partially

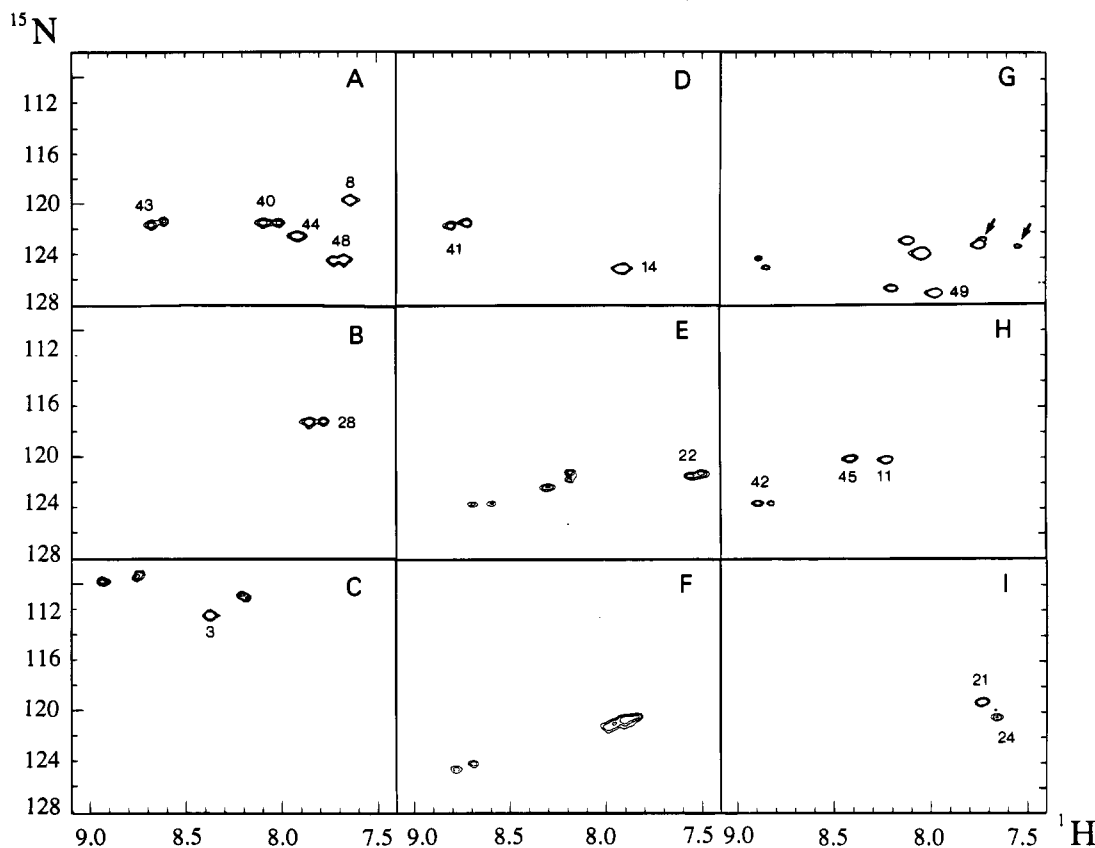


FIGURE 5:  $^1\text{H}/^{15}\text{N}$  HMQC spectra of various site-selectivity-labeled coat proteins in  $\text{SDS}-d_2\text{S}/\text{H}_2\text{O}$  buffer, pH 4.5,  $45^\circ\text{C}$ . (A) Lysine; (B) methionine; (C) glycine; (D) leucine; (E) isoleucine; (F) valine; (G) alanine; (H) phenylalanine; (I) tyrosine. Spectra were collected as described under Methods with 32–64 transients/increment.

assigned  $^1\text{H}/^{15}\text{N}$  HMQC spectrum as a guide, completion of the amide  $^1\text{H}$  and  $^{15}\text{N}$  chemical shift assignments becomes straightforward. For the extended regions at the N- and C-termini of the molecule (Henry et al., 1987a,b; Bogusky et al., 1988),  $\text{C}_\alpha\text{H}$  to  $\text{NH}$  ( $i + i + 1$ ) connectivities are prominent. Observation of the very narrow resonances (Figure 1C) required a long mixing time (200 ms), but under these conditions, sequential connectivities extending from alanine-1 to alanine-9 and from threonine-46 to serine-50 were located (not shown). Most of these peaks are quite intense in the  $^1\text{H}/^{15}\text{N}$  HMQC spectrum (Figure 4a). A notable exception is glutamic acid-2 which is partially saturated at pH 4.5. The amide proton closest to the N-terminus of a protein is unusually labile due to strong inductive effects from the positive charge at the  $\alpha$ -amino group (Molday et al., 1972; Henry et al., 1987b). The narrow doublet expected for the amide proton of glutamic acid-2 is present when the exchange rate is reduced by lowering either the pH or the temperature (Figure 1C, inset). It should be stressed that none of these  $\text{C}_\alpha\text{H}$  assignments were known previously, but they are obtained as a result of connecting the amide protons during the sequential assignment procedure.

Most of the remaining amide assignments were made using the strong  $\text{NH}$  to  $\text{NH}$  ( $i, i + 1$ ) NOEs which, at short mixing times, are characteristic of  $\alpha$ -helical structure (Wüthrich, 1986). The amide region of the NOESY spectrum of M13 coat protein is quite crowded, but the problem can be simplified by recording spectra in  $^2\text{H}_2\text{O}$  so that only the slowly exchanging amide protons are present. Figure 6 shows a NOESY spectrum obtained under sample conditions similar to those of Figures 2B and 4b. Three continuous sequences, V31-I32-V33, A35-T36-I37-G38, and I39-K40-L41, were identified readily with reference to the equivalent HMQC spectrum. The gaps in the sequence occur in regions of ex-

tensive spectral overlap. Once the  $^{15}\text{N}/^1\text{H}$  chemical shifts of the valine and isoleucine residues have been established from site-selective labeling and HMQC experiments, the  $\beta$ -protons are readily located in the NOESY spectrum, and the direction of the sequence between valines-31 and -33 is easily established from  $\text{C}_\beta\text{H}$  to  $\text{NH}$  ( $i, i + 1$ ) connectivities (Englander & Wand, 1987). The assignment of glycine-34 was obtained from continuing the  $\text{C}_\beta\text{H}$  to  $\text{NH}$  ( $i, i + 1$ ) sequence in the same NOESY spectrum. Location of the valine  $\beta$ -protons allows resolution and identification of the overlapping amides of valines-29, -30, and -31. In general, after the amide nitrogen and proton resonances had been assigned,  $\text{NH}$  to  $\text{C}_\beta\text{H}$  NOEs were easily identified and  $\text{C}_\beta\text{H}$  to  $\text{NH}$  ( $i, i + 1$ ) connectivities provided additional support to many of the sequential assignments. Qualitatively identical amide connectivities were observed at mixing times of either 50 or 100 ms.

Assignment of the slowly exchanging residues is now complete; they occur in a continuous sequence of 15 amides extending from methionine-28 to phenylalanine-42 (Figure 4b). Alanine-27 (discussed later) is present at lower intensity, and weak peaks corresponding to tryptophan-26, lysine-43, lysine-44, and phenylalanine-45 can also be seen if the vertical scale is increased (not shown). The hydrogen exchange properties of the coat protein are summarized in Figure 8.

NOESY spectra were also recorded on samples in which the slowly exchanging protons of the hydrophobic core were selectively deuterated (see Methods). With reference to the HMQC spectrum, strong sequential  $\text{NH}$  to  $\text{NH}$  ( $i, i + 1$ ) NOEs were easily identified at the C-terminal end of the protein (lysine-43 to serine-47), and cross-peaks connecting tyrosine-24 to a glycine and an alanine residue allowed the assignment of glycine-23 and alanine-25. Many strong sequential  $\text{NH}$  to  $\text{NH}$  NOEs are also observed in the N-terminal region (see



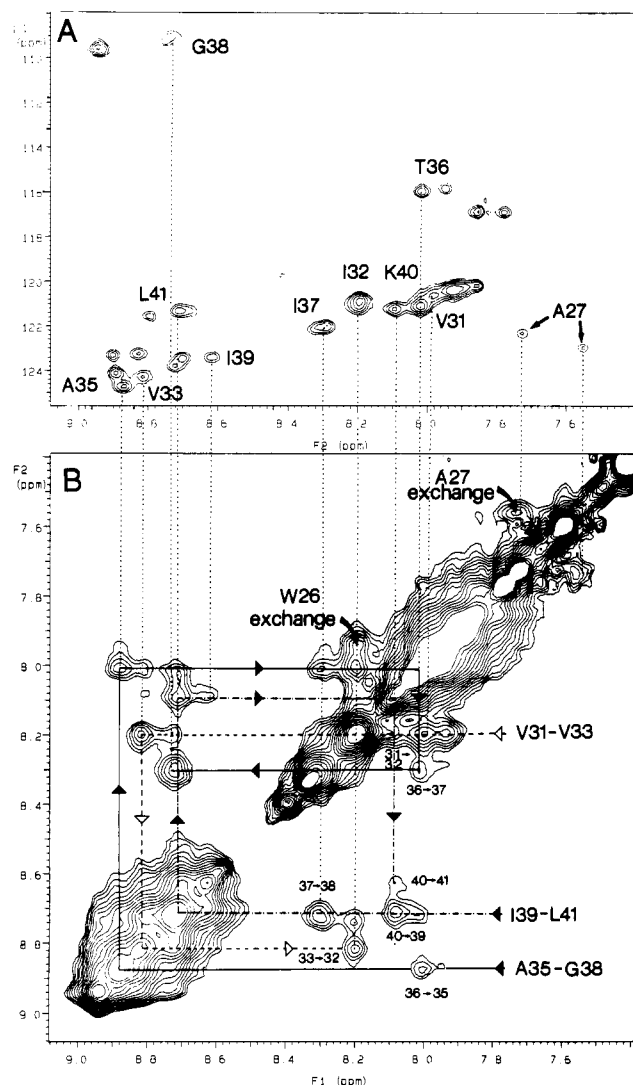


FIGURE 6: Assignment of the amide  $^1\text{H}$  and  $^{15}\text{N}$  resonances of the slowly exchanging region of M13 coat protein [(A) MVVVIVGATIGIKLF] using (A)  $^1\text{H}/^{15}\text{N}$  HMQC and (B) NOESY spectra (96 transients/increment) recorded in  $^2\text{H}_2\text{O}$  buffer and SDS- $d_{25}$  micelles. The HMQC spectrum was recorded after approximately 2-h equilibration in  $^2\text{H}_2\text{O}$  at  $45^\circ\text{C}$ , whereas the NOESY spectrum was acquired after a period of 36 h in  $^2\text{H}_2\text{O}$  at  $45^\circ\text{C}$ . The mixing time was 100 ms. Three continuous sequences of  $\text{NH}(i)$  to  $\text{NH}(i+1)$  NOEs were identified with the help of the HMQC spectrum: valine-31 to valine-33 (---), alanine-35 to glycine-38 (—), and isoleucine-39 to leucine-41 (---). In addition, exchange cross-peaks were observed between the well-separated amide protons of tryptophan-26 (visible in the HMQC spectrum at high vertical scale) and alanine-27 in the two forms of the protein. These amides are partially exchanged in both spectra.

below).

HMQC and NOESY may be combined directly into a single experiment (HMQC-NOESY; Shon & Opella, 1988; Gronenborn et al., 1989) in which interproton NOEs are transferred to an amide nitrogen atom, resulting in NOESY cross-peaks in the HMQC spectrum. This proved very useful for assignment of the remaining resonances of the N-terminal region where relatively few of the  $^{15}\text{N}$  resonances were assigned directly and unambiguous sequential tracing through the NOESY spectrum was not possible. All of the NOEs in the HMQC-NOESY spectrum (Figure 7) arise from sequential amide connectivities in the N-terminal region of the coat protein, extending from alanine-7 to threonine-19. The disadvantage of this experiment is that the improved resolution provided by the  $^{15}\text{N}$  dimension is offset by reduced sensitivity.

NOE cross-peaks from the hydrophobic region of the coat protein were not observed in the HMQC-NOESY spectrum because they are much weaker than those of the N-terminal domain as a result of broader line widths, resonance splitting, and exchange between monomers (discussed later).

The sequential assignment procedure allowed identification of most of the amide proton and nitrogen atoms in M13 coat protein. The remainder all lie between glutamic acid-20 and alanine-27, a region of the molecule in which the characteristic interproton NOEs are often missing. Assignment of alanine-25 (above) limits alanine-27 to the widely separated pair of alanine resonances discussed earlier and indicated by arrows in Figure 5G. The ring system of the single tryptophan-26 is easily identified from NOESY and COSY spectra [see also Cross and Opella (1981)], and the tryptophan-26 backbone NH was subsequently assigned from NOEs to the indole ring, observable at long mixing time. Like alanine-27, this residue also gives rise to a pair of well-separated resonances. The last residue, glutamic acid-20, was assigned to the only remaining resonance, which is close to lysine-44 in Figure 4a. The amide proton and nitrogen resonance frequencies are summarized in Table I.

**Inequivalence of the Coat Protein Monomers.** We have noted previously that a number of backbone carbonyl  $^{13}\text{C}$  and amide  $^1\text{H}$  resonances undergo a small splitting (Henry & Sykes, 1990c). The two peaks are always of similar intensity and line width, and the full extent of this phenomenon can now be appreciated (Figure 4a). The effect is most obvious in the  $^1\text{H}$  dimension, where the frequency difference is typically about 0.08 ppm (e.g., phenylalanine-42, threonine-36, methionine-28), although sometimes the  $^{15}\text{N}$  dimension is also involved (e.g., alanine-35, valine-33). Resonance splitting is a feature of the hydrophobic core and the C-terminal region, affecting about 22 out of 36 residues between isoleucine-22 and lysine-48 (indicated with triangles in Figure 8). None of the N-terminal resonances are affected under these conditions (although the backbone amide of leucine-14 and the side chain amide of glutamine-15 resolve into two peaks at lower temperature). Apart from this overall spatial segregation, no general patterns emerge in the frequency of distribution. The frequency difference between the two resonances is generally small with respect to the overall chemical shift dispersion, leading to the conclusion that the conformational difference must also be small; the exceptions are the adjacent residues, tryptophan-26 and alanine-27. Resonance splitting is also evident for the side chain amide of tryptophan-26 [see also O'Neil and Sykes (1989a)].

It is expected that the two forms of the coat protein should be in equilibrium. Although exchange between conformers is clearly slow on the chemical shift time scale, evidence for exchange on a time scale of approximately 1 s or less can be found in the NOESY spectra. The large separation of the amide proton resonances arising from tryptophan-26 and alanine-27 leads to exchange cross-peaks which are well off the diagonal (Figure 6). These are present in spite of the fact that both amides have largely exchanged with the deuterated solvent; in  $\text{H}_2\text{O}$ , these cross-peaks are very intense. The HMQC-NOESY spectrum shows exchange cross-peaks between resonances that are split in both the  $^1\text{H}$  and  $^{15}\text{N}$  dimensions, e.g., alanine-35 (Figure 7). The presence of chemical exchange decreases the intensity of the NOESY cross-peaks in the amide proton region.

## DISCUSSION

Structural studies of integral membrane proteins still present a considerable challenge [see Pattus (1990) for a recent re-

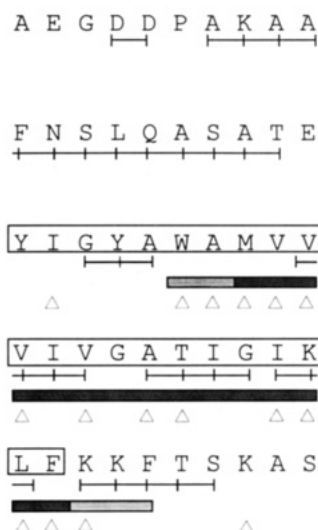
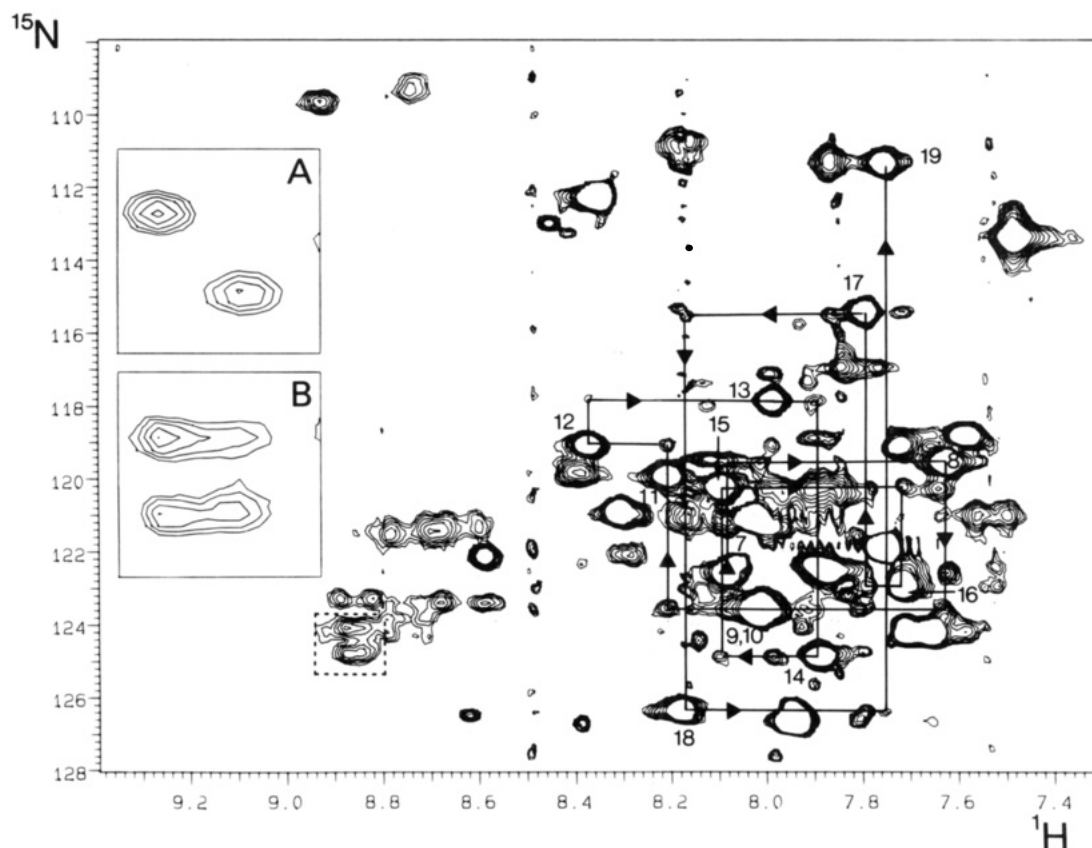


FIGURE 8: Sequence of M13 coat protein (van Wezenbeek et al., 1980) showing the region of slowly exchanging amide protons (stippled region), the location of NH (*i*) to NH (*i*+1) NOEs observed at either 50- or 100-ms mixing times, and the occurrence of double peaks ( $\Delta$ ). The hydrophobic sequence is indicated by a box.

the NH to C $\alpha$ H region, where the coupling constant is only about 4 Hz in an  $\alpha$ -helix. As a result, identification of amino acid spin systems from homonuclear scalar connectivities undergoes a dramatic rise in difficulty as molecular size increases. All these problems are applicable to SDS-solubilized M13 coat protein, which has an apparent molecular weight of 27 000 (Makino et al., 1975). The presence of two conformational forms, and the exchange between them, introduces extra complexity and decreases the intensity of affected resonances. Nevertheless, high-quality NOESY spectra are readily obtained, and the structural information is available for extraction if an appropriate assignment strategy can be found.

Several types of NMR experiments have been devised recently to tackle the problems presented by larger molecules, including isotope editing ( $^{13}\text{C}$  and  $^{15}\text{N}$ ), multidimensional NMR, and dilution of the proton spins by selective or random fractional deuteration [e.g., see Griffey et al. (1986), Fesik et al. (1988), Marion et al. (1989), Ikura et al. (1990), LeMaster and Richards (1987), Arrowsmith et al. (1990), and Shon et al. (1991)]. An "amide-directed" strategy, based on assignment of the  $^1\text{H}/^{15}\text{N}$  HMQC spectrum, was successful with staphylococcal nuclease ( $M_r = 17\,400$ ; Torchia et al., 1988, 1989) and  $\text{T}_4$  lysozyme ( $M_r = 18\,700$ ; McIntosh et al., 1990). This experiment is particularly effective with large molecules because it relies on the large coupling constant between the proton and the bonded heteroatom.

In conventional assignment procedures, COSY or HOHAHA spectra are used to determine residue type, and specific assignments are made subsequently on the basis of characteristic NOEs between adjacent residues. The "amide-

directed" approach, by contrast, relies on site-selective  $^{15}\text{N}$  labeling to determine residue type, and this information is used for sequential assignment of the NOESY spectrum. Independent, directly-obtained  $^{15}\text{N}$  assignments of specific amides are very helpful, as they limit our reliance on the otherwise error-prone sequential assignment procedure.  $^{15}\text{N}$  assignments can often be determined unambiguously with relative ease, for example, by double-labeling or by enzyme digestion. Existing knowledge of the exchange rates of many amide protons from  $^{13}\text{C}$  carbonyl carbon isotope shift experiments in 1:1  $^1\text{H}_2\text{O}/^2\text{H}_2\text{O}$  (Henry et al., 1987b; Henry & Sykes, unpublished results) was particularly useful for M13 coat protein, as it transfers information across a peptide bond. The reverse principle was applied by Tuchsén and Hansen (1988) to assign carbonyl carbons in the basic pancreatic trypsin inhibitor. Thus, in the absence of adequate COSY data, the HMQC spectrum assigned to residue type can serve as an invaluable guide for the identification of NOEs to the amide protons [NH to NH ( $i, i+1$ ),  $\text{C}_\alpha\text{H}$  to NH ( $i, i$  or  $i, i+1$ ), and  $\text{C}_\beta\text{H}$  to NH ( $i, i$  or  $i, i+1$ )]. In the case of M13 coat protein, many  $\text{C}_\beta\text{H}$  to NH ( $i, i$ ) and ( $i, i+1$ ) NOEs could be obtained, but with the exception of the mobile termini, identification of  $\text{C}_\alpha\text{H}$  protons was more difficult. The  $^1\text{H}$  and  $^{15}\text{N}$  assignments provide other information about the coat protein, such as complete identification of the very mobile residues and the slowly exchanging amide protons. It also reveals the full extent of the phenomenon of resonance "splitting" which can be used as a basis for the study of intermolecular association.

**Mobile Terminal Residues.** It has been recognized for some time from  $^{13}\text{C}$  and  $^{15}\text{N}$  NMR experiments that residues near the termini of M13 coat protein exhibit relatively narrow lines due to motions of the protein backbone (Cross & Opella, 1980; Henry et al., 1987a; Bogusky et al., 1988) and these can now be located precisely (Figure 1C). Because all of the backbone motion occurs about the  $\text{C}_\alpha\text{--N}$  and  $\text{C}_\alpha\text{--C}_\beta$  bonds, it is simplest to consider the mobility of the peptide bond as an intact unit. Alanine-1 has no amide, but extremely narrow lines can be recognized for the peptide bonds of alanine-1 (CO)–glutamic acid-2 (NH) (at low pH), glutamic acid-2 (CO)–glycine-3 (NH), and glycine-3 (CO)–aspartic acid-4 (NH) at the N-terminus of the coat protein, and at alanine-49 (CO)–serine-50 (NH) at the C-terminus. Approximately equivalent in line width, and less prominent, are the aspartic acid-4 (CO)–aspartic acid-5 (NH) and lysine-48 (CO)–alanine-49 (NH) bonds. Nevertheless, the amide of lysine-48 still has sufficient mobility to give rise to a negative  $^{15}\text{N}$ NOE, and it is clear that gradients of mobility occur at both ends of the protein. However, contrary to the conclusions of Bogusky et al. (1988), our data suggest that the gradient at the N-terminus of the protein is considerably less steep than that at the C-terminus (see later).

**Amide Exchange.** Measurement of the exchange rates of backbone amide protons with the solvent is a potential source of both structural and dynamic information (Englander & Kallenbach, 1984). Using one-dimensional  $^1\text{H}$  NMR, a set of about 16 slowly exchanging amide protons was identified by multiple exponential analysis of the decay of the amide proton envelope as a function of pH\* when protonated protein was dissolved in  $^2\text{H}_2\text{O}$  buffer (O'Neil & Sykes, 1988).  $^1\text{H}/^{15}\text{N}$  HMQC spectroscopy of  $^{15}\text{N}$ -labeled coat protein has allowed both the resolution of the slowly exchanging protons and their assignment; they occur in a continuous sequence of 15 residues, extending from methionine-28 to phenylalanine-42.

The upper limit of the exchange rate of these amides can be calculated approximately. Assuming  $\geq 90\%$  of the signal

intensity to remain after 12 h (2 h of equilibration, 10 h of data collection), the amide exchange rate  $k_{\text{ex}} \leq 2.5 \times 10^{-6} \text{ s}^{-1}$ . As  $k_{\text{ex}}$  is determined both by temperature and by pH, it is usually expressed in terms of the rate of exchange of a model compound, the unstructured, non-H-bonded polypeptide poly(DL-alanine), under similar conditions (Englander & Kallenbach, 1984). The slowly exchanging amides in M13 coat protein are thus calculated to be at least  $10^5$ -fold slower than poly(DL-alanine) [see also O'Neil and Sykes (1988)]. Detailed kinetics of several individual slowly exchanging amides have been presented previously; leucine-41 and a valine residue which can now be identified as valine-33 are about ( $1 \times 10^6$ )-fold and ( $7 \times 10^6$ )-fold slower than poly(DL-alanine), respectively<sup>2</sup> (Henry & Sykes, 1990b). The pH minimum of the slowly exchanging amides is between 4 and 4.5, i.e., close to the operating pH of these experiments. The effect of the hydrophobic environment of the micelle on amide proton exchange rates has been discussed in detail by O'Neil and Sykes (1989) for model peptides and by Henry and Sykes (1990) for M13 coat protein. The continuous sequence of slowly exchanging residues does not correspond exactly to the 19 residues of the hydrophobic core; as well as being shorter, it is shifted toward the C-terminal end of the molecule. At the ionic strength of these experiments, isolated SDS micelles are smaller in diameter than the width of the *E. coli* inner membrane, which may account for the difference. The micelle almost certainly contributes to the stability of the coat protein structure and may be responsible for maintenance of the dimeric state.

**Model of the Coat Protein Dimer.** In a regular  $\alpha$ -helix, successive amides are approximately parallel, leading to strong NOEs between the amide protons which are only 2.8 Å apart. Extended chains or  $\beta$ -sheet, by contrast, have adjacent amides directed away from one another (4.4 Å apart), providing a distinct difference between these two major elements of secondary structure which may be recognized qualitatively. Prominent NOEs between successive amides, such as those observed in the coat protein, are indicative of helical structure. In the absence of  $\text{C}_\alpha\text{H}$  assignments, we cannot locate the medium-range connectivities which confirm the helical turn of the polypeptide chain [i.e.,  $\text{C}_\alpha\text{H}$  to NH ( $i, i+3$ ),  $\text{C}_\alpha\text{H}$  to  $\text{C}_\beta\text{H}$  ( $i, i+3$ ); Wüthrich, 1986]. Nevertheless, we can combine our existing NOE data with other evidence to produce a realistic model for the SDS-solubilized M13 coat protein dimer.

SDS-bound M13 coat protein is proposed to consist of two  $\alpha$ -helices linked by a short region of uncertain conformation. The longer C-terminal helix extends through much of the hydrophobic section and the basic region of the protein, ending near the C-terminus. This part of the molecule is very stable and held together by hydrophobic interactions between the monomers and probably to some extent by interactions with the detergent micelle. The N-terminal helix is suggested to reside outside the micelle and appears to be more structurally labile. It is possible to remove this region of the protein with proteinase K (Henry et al., 1987a,b). As has been noted earlier, the very ends of the polypeptide chain are disordered.

Evidence for the C-terminal helix is provided by the continuous sequence of slowly exchanging amide protons and a number of sequential NH to NH connectivities. The start of the helix is not easily defined. The first slowly exchanging amide is methionine-28, whereas due to spectral overlap, the

<sup>2</sup> The calculated exchange rates are not corrected for neighboring residue effects (Molday et al., 1972). There is an error in Table I of Henry and Sykes (1990a); the value given for the retardation ( $1/K_{\text{op}}$ ) of leucine-41 should be  $1.1 \times 10^6$  not  $1.1 \times 10^4$ .

first observable NH to NH NOE is between valine-31 and isoleucine-32. Our analysis of the NOEs in this region relied on the use of the slowly exchanging amides to edit the NOESY spectrum, which naturally limits the result; it is conceivable that the helix may extend further in the N-terminal direction. It should also be remembered that the first four amides of an  $\alpha$ -helix are not hydrogen-bonded to residues within the helix. No evidence of extended chain or  $\beta$ -sheet has been observed in the region of the slowly exchanging amides. The steep increase in amide exchange rate (measured previously) upon approach of the C-terminus has been explained in terms of dynamic helical fraying (Henry et al., 1987b). In support of this interpretation, weak NOEs characteristic of the extended chain (arising from the short distance between an NH and the  $\text{C}_\alpha\text{H}$  of the preceding residue; Wüthrich, 1986) are first observed at threonine-46. These intensify progressively as the NH to NH NOEs weaken upon approach of the C-terminal residue.

The character of the N-terminal helix appears to be quite different. Strong NH ( $i$ ) to NH ( $i+1$ ) NOEs are present between alanine-7 and threonine-19 (equivalent to 3.5 helical turns); however, the amide exchange rates are all quite fast, and the N-terminal region appears to be in a state of relatively rapid dynamic flux. Although we have previously suggested this region of the molecule to be rigid on the time scale of  $^{13}\text{C}$  relaxation at room temperature (Henry et al., 1986), several lines of evidence lead us to conclude that a limited amount of backbone motion may be present at 45 °C. In particular, the line widths of the N-terminal  $^1\text{H}$  resonances in Figures 2 and 4 are narrower than those of the rest of the molecule, and much intensity is missing from a spectrum of uniformly  $^{15}\text{N}$ -labeled coat protein recorded in the presence of the  $^{15}\text{N}$  NOE. The latter observation suggests that a significant portion of the signal is lost due to small negative  $^{15}\text{N}$  NOEs (the situation observed for lysine-8 in Figure 3d). The experiment is difficult to interpret, however, as the uniform  $^{15}\text{N}$ -labeled spectrum is dominated by the large negative NOEs arising from the very mobile residues at the termini.

Under the conditions of our experiments, 2 M13 coat protein monomers are associated with approximately 60 SDS molecules (Makino et al., 1975). The small size of the micelle necessitates extensive interactions between individual protein monomers; in fact, the monomers are very difficult to dissociate (Nozaki et al., 1978). We propose that the M13 coat protein dimer consists of a pair of helical structures, described above, associated with a single SDS micelle. Lacking evidence to the contrary, we consider the monomers to be aligned in a parallel fashion, their orientation in the intact phage.

On the basis of NH to NH NOEs, Shon et al. (1991) proposed a similar model for the 46-residue coat protein of the related phage Pf1 solubilized in dodecylphosphocholine micelles; 2 helices (residues 6–13 and 19–42) are connected by a short loop. In contrast with M13, the Pf1 coat protein is believed to be monomeric. Solid-state NMR experiments on Pf1 coat protein reconstituted into phospholipid bilayers showed the N-terminal helix to lie parallel to the surface of the bilayer. The relative orientation of the two helices of M13 coat protein is not known, but it is certainly possible that the N-terminal helix is similarly associated with the surface of the SDS micelle.

**Chemical Shifts.** A number of interesting structural correlations are beginning to emerge from the rapidly expanding database of proton chemical shifts. Amide protons in an  $\alpha$ -helix resonate, on average, 0.2–0.3 ppm upfield from the random-coil position for any given amino acid residue whereas

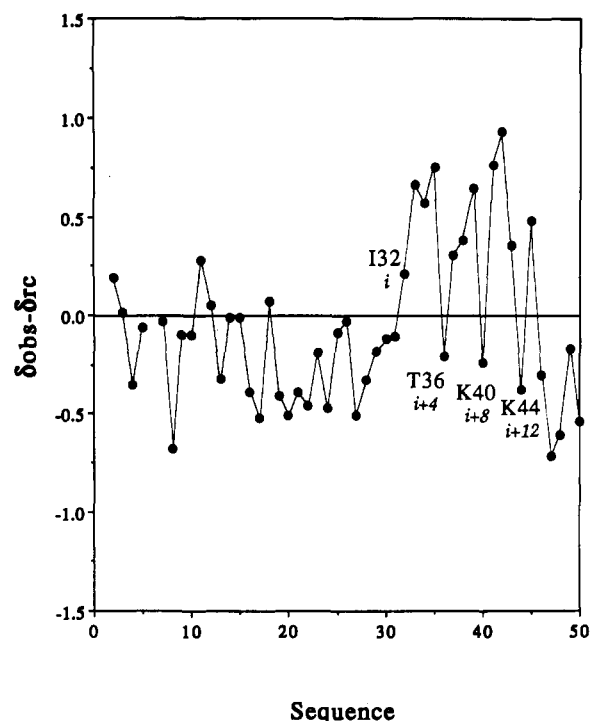


FIGURE 9: Plot of the difference between observed and random-coil amide proton resonance frequencies ( $\delta_{\text{obs}} - \delta_{\text{rc}}$ ) for M13 coat protein in SDS micelles.  $\delta_{\text{rc}}$  values were taken from Wishart et al. (1991). The average frequency was taken in the case of "double" resonances. This chemical shift difference is small compared with the overall dispersion.

amides in a  $\beta$ -sheet are shifted downfield by a similar amount (Williamson, 1990). Unfortunately, amide chemical shifts are not as reliable an indicator of secondary structure as the  $\text{C}_\alpha\text{H}$  resonance frequencies (Szilagyi & Jardetzky, 1989; Wishart et al., 1991) as amides in general show a broader frequency distribution with substantial overlap between the two populations; however, the amide proton frequency appears to be sensitive to N–H bond length, which may in turn be a function of hydrogen-bond strength (Wagner et al., 1983).

Most of the amide proton resonances in SDS-solubilized M13 coat protein have negative secondary shifts ( $\delta_{\text{observed}} - \delta_{\text{random coil}}$ ), indicating high helical content (Figure 9). Between residues 1 and 25, the secondary shift tends to decrease (i.e., to become more negative), which is consistent with the proposed progressive increase in stability of the N-terminal helix. Amide exchange rates in this region follow the same general trend, becoming slower as the distance from the N-terminus increases (G. D. Henry and B. D. Sykes unpublished observations). In striking contrast, a number of amides in the hydrophobic region have large positive secondary shifts. Within this group (residues 32–44), there is a strong periodicity ( $i, i+4$ ), reminiscent of  $\alpha$ -helical coiled-coil proteins (Kuntz et al., 1991). The periodicity is independent of whether the resonance frequencies are plotted directly or as secondary shifts and continues for about three turns of an  $\alpha$ -helix.

Coiled coils are strongly amphiphilic, self-associating helices with hydrophilic and hydrophobic surfaces running along their length [see Cohen and Parry (1990)]. It has been suggested that the observed periodicity arises from distortions induced by curvature of helix (Kuntz et al., 1991) which in turn lead to differential hydrogen-bond lengths on the solvent-exposed and solvent-excluding surfaces. It is possible that the chemical shift periodicity in SDS-solubilized M13 coat protein arises from a similar distortion, which may be induced by the association of the monomers; however it is important to realize

that the chemical shift periodicity is not, in itself, evidence for helical structure or for dimer formation. The relevant region of the molecule is shifted toward the C-terminal end of the long micelle-binding helix. By analogy with the coiled-coil proteins, the most upfield-shifted amide protons (residues isoleucine-32, threonine-36, lysine-40, and lysine-44) would lie along the outer surface of the dimer. As far as can be judged from the published spectra, the micelle-solubilized coat protein of the related phage Pf1, which is thought to be monomeric, does not show any periodicity of the amide proton chemical shifts.

**Interactions in the Coat Protein Dimer.** We have noted previously that a number of backbone carbonyl carbon and amide proton resonances in M13 coat protein undergo small splittings (Henry & Sykes, 1990c). The full extent of this phenomenon can now be appreciated; 20–25 resonances between isoleucine-22 and lysine-48 (i.e., residues of the C-terminal helix or linker region) can be resolved into 2 peaks at 500 MHz. Multiple resonances have been observed recently for several proteins; for example, a substantial population of the *cis* conformer about a Gly–Pro bond in calbindin affected the resonance frequency of about half of the cross-peaks in the NH to C $\alpha$ H region of the COSY spectrum (Kordel et al., 1989), and an uncleaved methionine resonance at the N-terminus of cloned human thioredoxin influenced 28 out of 105 NH to C $\alpha$ H resonances (Forman-Kay et al., 1989). The pattern observed with M13 is different; most of the resonances appear as discrete “doublets”, for example, the lysine resonances in Figure 5A. As the frequency differences observed with M13 coat protein are small compared with the overall chemical shift dispersion (the only exceptions are tryptophan-26 and alanine-27), the resonances are of equal size, we have attributed this effect to a small conformational difference between the individual monomers of the M13 coat protein dimer (Henry & Sykes, 1990c). Such an effect could result from the packing of two parallel  $\alpha$ -helices. As would be expected on thermodynamic grounds, the observation of chemical exchange peaks in the NOESY spectra shows the two species to be in equilibrium.

**Other Models for the Coat Protein.** M13 coat protein is largely  $\alpha$ -helical in the intact phage (100%  $\alpha$  or  $\alpha$ -form; Marvin & Wachtel, 1976; Makowski, 1984; Nozaki et al., 1976, 1978; Opella et al., 1987) but is reported to undergo a large conformational change to a 50%  $\alpha$  or  $\beta$ -form upon either incorporation into lipid bilayers or solubilization in micelles of detergents such as deoxycholate or SDS (Nozaki et al., 1976, 1978; Dunker et al., 1979, 1981). The detergent-bound  $\beta$ -form has been proposed to possess varying amounts of  $\beta$ -sheet structure (Nozaki et al., 1978; Webster & Cashman 1981; Chamberlain et al., 1978; Grygon et al., 1988), and several models for the protein–detergent complex have been proposed. Our results, in contrast, suggest that the phage retains much of its helical structure upon dissociation into SDS and the conformational change upon solubilization is comparatively small.

#### ACKNOWLEDGMENTS

We thank Gerry McQuaid for constructing the  $^{15}\text{N}$  probe and for maintenance of the NMR spectrometers, Dr. Joel Weiner for his continued interest and for providing facilities and laboratory space for the growth of *E. coli* cells and phage purification, and the Medical Research Council of Canada for financial support.

#### REFERENCES

- Arrowsmith, C. H., Pachter, R., Altman, R. B., Iyer, S. B., & Jardetzky, O. (1990) *Biochemistry* 29, 6332–6341.
- Bax, A., Griffey, R. H., & Hawkins, B. L. (1983) *J. Magn. Reson.* 55, 301–315.
- Billeter, M., Braun, W., & Wüthrich, K. (1982) *J. Mol. Biol.* 155, 321–346.
- Bogusky, M. J., Tsang, P., & Opella, S. J. (1985a) *Biochem. Biophys. Res. Commun.* 127, 540–545.
- Bogusky, M. J., Leo, G. C., & Opella, S. J. (1988) *Proteins: Struct., Funct., Genet.* 4, 123–130.
- Bundi, A., & Wüthrich, K. (1979) *Biopolymers* 18, 285–297.
- Cavaliere, S. J., Goldthwaite, D. A., & Neet, K. E. (1976) *J. Mol. Biol.* 102, 713–722.
- Chang, C. N., Model, P., & Blobel, G. (1978) *Proc. Natl. Acad. Sci. U.S.A.* 75, 361–365.
- Cohen, C., & Parry, D. A. D. (1990) *Proteins: Struct., Funct., Genet.* 7, 1–15.
- Cross, T. A., & Opella, S. J. (1980) *Biochem. Biophys. Res. Commun.* 92, 478–484.
- Cross, T. A., & Opella, S. J. (1981) *Biochemistry* 20, 290–297.
- Cross, T. A., & Opella, S. J. (1985) *J. Mol. Biol.* 182, 367–381.
- Datema, K. P., Visser, A. J. W. G., van Hoek, A., Wolfs, C. J. A. M., Spruijt, R. B., & Hemminga, M. A. (1987) *Biochemistry* 26, 6145–6152.
- Deisenhofer, J., Epp, O., Miki, K., Huber, R., & Michel, H. (1985) *Nature* 318, 618–621.
- Dettman, H. D., Weiner, J. H., & Sykes, B. D. (1984) *Biochemistry* 23, 705–712.
- Doddrell, D. M., Pegg, D. T., & Bendall, M. R. (1982) *J. Magn. Reson.* 48, 323–327.
- Engelman, D. M., Goldman, A., & Steitz, T. (1982) *Methods Enzymol.* 88, 81–89.
- Englander, S. W., & Kallenbach, N. R. (1984) *Q. Rev. Biophys.* 16, 521–655.
- Englander, S. W., & Wand, A. J. (1987) *Biochemistry* 26, 5953–5958.
- Fasman, G. D., & Gilbert, W. A. (1990) *Trends Biochem. Sci.* 15, 89–92.
- Feeney, J., Partington, P., & Roberts, G. C. K. (1974) *J. Magn. Reson.* 13, 268–274.
- Fesik, S. W., Luly, J. R., Erickson, J. W., & Abad-Zapatero, C. (1988) *Biochemistry* 27, 8297–8301.
- Fodor, S. P. A., Dunker, A. K., Ng, Y. C., Carsten, D., & Williams, R. W. (1981) in *Bacteriophage Assembly*, p 441, Alan Liss Inc., New York.
- Forman-Kay, J. D., Clore, G. M., Driscoll, P. C., Wingfield, P., Richards, F. M., & Gronenborn, A. M. (1989) *Biochemistry* 28, 7088–7097.
- Griffey, R. H., Redfield, A. G., Loomis, R. E., & Dalquist, F. W. (1985) *Biochemistry* 24, 817–822.
- Gronenborn, A. M., Bax, A., Wingfield, P. T., & Clore, G. M. (1989) *FEBS Lett.* 243, 93–98.
- Grygon, C. A., Perno, J. R., Fodor, S. P. A., & Spiro, T. G. (1988) *BioTechniques* 6, 50–55.
- Henderson, R., & Unwin, P. N. T. (1975) *Nature* 257, 28–32.
- Henderson, R., Baldwin, J. M., Ceska, T. A., Zemlin, F., Beckman, E., & Downing, K. H. (1990) *J. Mol. Biol.* 213, 899–929.
- Henry, G. D., & Sykes, B. D. (1990a) *Biochem. Cell Biol.* 68, 318–329.
- Henry, G. D., & Sykes, B. D. (1990b) *Biochemistry* 29, 6303–6313.
- Henry, G. D., & Sykes, B. D. (1990c) *J. Mol. Biol.* 212, 11–14.
- Henry, G. D., Weiner, J. H., & Sykes, B. D. (1986) *Biochemistry* 25, 590–598.

- Henry, G. D., Weiner, J. H., & Sykes, B. D. (1987a) *Biochemistry* 26, 3619–3626.
- Henry, G. D., Weiner, J. H., & Sykes, B. D. (1987b) *Biochemistry* 26, 3626–3634.
- Jahnig, F. (1990) *Trends Biochem. Sci.* 15, 93–95.
- Kleffel, B., Garavito, R. M., Baumeister, W., & Rosenbusch, J. P. (1985) *EMBO J.* 4, 1589–1592.
- Kordel, J., Forsen, S., & Chazin, W. (1989) *Biochemistry* 28, 7065–7074.
- Kuhn, A., Zhu, H.-Y., & Dalbey, R. E. (1990) *EMBO J.* 9, 2385–2389.
- Kuntz, I. D., Kosen, P. A., & Craig, E. C. (1991) *J. Am. Chem. Soc.* 113, 1406–1408.
- LeMaster, D. M., & Richards, F. M. (1988) *Biochemistry* 27, 142–150.
- Leo, G. C., Colnago, L. A., Valentine, K. G., & Opella, S. J. (1987) *Biochemistry* 26, 854–862.
- Makino, S., Woolford, J. L., Tanford, C., & Webster, R. E. (1975) *J. Biol. Chem.* 250, 4327–4332.
- Marion, D., Driscoll, P. C., Kay, L. E., Wingfield, P. T., Bax, A., Gronenborn, A. M., & Clore, G. M. (1989) *Biochemistry* 28, 6150–6156.
- McIntosh, L. P., Wand, A. J., Lowry, D. F., Redfield, A. G., & Dahlquist, F. W. (1990) *Biochemistry* 29, 6341–6362.
- Michel, H. (1982) *J. Mol. Biol.* 158, 567–572.
- Miller, J. H. (1972) *Experiments in Molecular Genetics*, Cold Spring Harbor Laboratory, Cold Spring Harbor, NY.
- Molday, R. S., Englander, S. W., & Kallen, R. G. (1972) *Biochemistry* 11, 150–158.
- Morris, G. A. (1980) *J. Am. Chem. Soc.* 102, 428–429.
- Müller, L. (1979) *J. Am. Chem. Soc.* 101, 4481–4484.
- Nozaki, Y., Chamberlain, B. K., Webster, R. E., & Tanford, C. (1976) *Nature (London)* 259, 335–337.
- Nozaki, Y., Reynolds, J. A., & Tanford, C. (1978) *Biochemistry* 17, 1239–1246.
- O'Neil, J. D. J., & Sykes, B. D. (1988) *Biochemistry* 27, 2753–2762.
- O'Neil, J. D. J., & Sykes, B. D. (1989a) *Biochemistry* 28, 699–707.
- O'Neil, J. D. J., & Sykes, B. D. (1989b) *Biochemistry* 28, 6736–6745.
- Pattus, F. (1990) *Curr. Opin. Cell Biol.* 2, 681–685.
- Schiksnis, R. A., Bogusky, M. J., Tsang, P., & Opella, S. J. (1987) *Biochemistry* 26, 1373–1381.
- Shaka, A. J., Keeler, J., Frenkiel, T., & Freeman, R. (1983) *J. Magn. Reson.* 52, 335–338.
- Shon, K.-J., & Opella, S. J. (1989) *J. Magn. Reson.* 82, 193–197.
- Shon, K.-J., Kim, Y., Colnago, L. A., & Opella, S. J. (1991) *Science* 252, 1303–1305.
- Spruijt, R. B., Wolfs, C. J. A. M., & Hemminga, M. A. (1989) *Biochemistry* 28, 9158–9165.
- Srinivasan, P. R., & Lichter, R. L. (1977) *J. Magn. Reson.* 28, 227–234.
- States, D. J., Haberkorn, R. A., & Ruben, D. J. (1982) *J. Magn. Reson.* 48, 286–296.
- Szilagyi, L., & Jardetzky, O. (1989) *J. Magn. Reson.* 83, 441–449.
- Tanford, C., & Reynolds, J. A. (1976) *Biochim. Biophys. Acta* 457, 133–170.
- Torchia, D. A., Sparks, S. W., & Bax, A. (1988) *Biochemistry* 27, 5135–5141.
- Torchia, D. A., Sparks, S. W., & Bax, A. (1989) *Biochemistry* 28, 5509–5524.
- Tuchsen, E., & Hansen, P. E. (1988) *Biochemistry* 27, 8568–8576.
- van Wezenbeek, P. M. F. G., Hulsebos, T. J. M., & Schoenmakers, J. G. G. (1980) *Gene* 11, 129–148.
- Wagner, G., Pardi, A., & Wüthrich, K. (1983) *J. Am. Chem. Soc.* 105, 5948–5949.
- Webster, R. E., & Cashman, T. S. (1988) in *The Single-stranded DNA Phages* (Denhardt, D. T., Dressler, D., & Ray, D., Eds.) pp 557–569, Cold Spring Harbor Laboratory, Cold Spring Harbor, NY.
- Weiss, M. S., Abele, U., Weckesser, J., Welte, W., Schlitz, E., & Schulz, G. E. (1991) *Science* 254, 1627–1630.
- Wickner, W. (1975) *Proc. Natl. Acad. Sci. U.S.A.* 72, 4749–4753.
- Wickner, W. (1980) *Science* 210, 861–863.
- Wickner, W. (1988) *Biochemistry* 27, 1107–1114.
- Williams, R. W., & Dunker, A. K. (1977) *J. Biol. Chem.* 252, 6253–6255.
- Williamson, M. P. (1991) *Biopolymers* 29, 1423–1431.
- Wilson, M. L., & Dahlquist, F. W. (1985) *Biochemistry* 24, 1920–1928.
- Wishart, D. S., Sykes, B. D., & Richards, F. M. (1991) *J. Mol. Biol.* 222, 311–333.
- Woolford, J. L., & Webster, R. E. (1975) *J. Biol. Chem.* 250, 4333–4339.
- Wüthrich, K. (1986) in *NMR of Proteins and Nucleic Acids*, Wiley, New York.
- Wüthrich, K. (1989) *Science* 243, 45–50.